

Neutron-radiation-induced flux pinning in Gd-doped $\text{YBa}_2\text{Cu}_3\text{O}_{7-x}$ and $\text{GdBa}_2\text{Cu}_3\text{O}_{7-x}$

K. E. Sickafus, J. O. Willis,* P. J. Kung, W. B. Wilson, D. M. Parkin, M. P. Maley,
F. W. Clinard, Jr., C. J. Salgado, R. P. Dye, and K. M. Hubbard

Los Alamos National Laboratory, Los Alamos, New Mexico 87545

(Received 13 December 1991; revised manuscript received 30 March 1992)

The critical current density J_c in $\text{Y}_{0.9}\text{Gd}_{0.1}\text{Ba}_2\text{Cu}_3\text{O}_{7-x}$ was found to increase relative to the unirradiated value following neutron irradiations in a mixed-spectrum reactor (total neutron fluences ranged between 1×10^{17} and 2×10^{18} n/cm²). Additional neutron irradiations of structurally similar $\text{GdBa}_2\text{Cu}_3\text{O}_{7-x}$ were carried out in either a highly thermalized or a pure fast-neutron environment (in the same reactor). This was done to determine whether enhancements in J_c are to be attributed to defects arising from interactions with thermal neutrons ($E_n \sim 0.025$ eV) or with fast neutrons ($E_n > 0.1$ MeV). Magnetic-hysteresis measurements on these samples indicate that flux pinning (and thereby J_c) is enhanced by fast-neutron irradiation, but not by thermal-neutron irradiation. On the other hand, the critical temperature T_c is significantly altered by exposure both to thermal and fast neutrons. It is proposed that thermal neutrons induce the formation of Frenkel pair defects on the rare-earth sublattice, but that these point defects do not serve as effective flux-pinning centers.

INTRODUCTION

The study of neutron irradiation effects in high-temperature superconductors (HTSC) is currently an area of extensive investigations in both polycrystalline¹ and single-crystal materials.²⁻⁵ An important result of this activity is the report of enhanced critical current density (J_c) in the superconductor $\text{YBa}_2\text{Cu}_3\text{O}_{7-x}$ upon exposure to fast neutrons.⁶ At low neutron fluence, the enhancement in J_c is attributed to the creation of defects in the crystalline lattice that act as pinning sites for the magnetic flux.⁷ Higher neutron fluences produce more damage to the crystal lattice and deleterious effects on the superconducting properties.⁸

The purpose of the study presented here is to distinguish the roles of thermal and fast neutrons in inducing damage in HTSC materials containing gadolinium (Gd), and the role of such damage on superconducting properties. The compositions $\text{Y}_{0.9}\text{Gd}_{0.1}\text{Ba}_2\text{Cu}_3\text{O}_{7-x}$ and $\text{GdBa}_2\text{Cu}_3\text{O}_{7-x}$ were chosen for this study in order to initiate defects on the rare-earth sublattice. This is achieved as a result of the very large cross section for thermal-neutron capture of the Gd dopant ($\langle \sigma_\gamma \rangle \sim 5 \times 10^4$ b). Upon neutron capture, the Gd nuclei relax to their ground states by γ -ray emission. The momentum transfer to the recoiling Gd nucleus by this mechanism can result in the ejection of the Gd nucleus from its lattice site. In a reactor with a large thermal component in its neutron spectrum, a substantial fraction of defects are produced by this mechanism as compared to fast-neutron-induced defects, where the cross sections for neutron-nucleon interaction are, with a few exceptions, between 1 and 10 b.⁹ Results are compared to other HTSC neutron damage studies.

EXPERIMENTAL PROCEDURE

Powders of Gd_2O_3 , Y_2O_3 , BaO , and CuO were ball-milled together and pressed into disks approximately 3

cm in diameter and 4 mm thick. The pellets were subjected to a series of heat treatments in one atmosphere of oxygen as follows: 300–775 K in 5 h, 755–1175 K in 6 h, hold at 1175 K for 24 h, 1175–775 K in 24 h (the oxygenation step), and 775–300 K in 5 h.

The composition of the Gd-doped sintered pellets were nominally $\text{Y}_{0.9}\text{Gd}_{0.1}\text{Ba}_2\text{Cu}_3\text{O}_{7-x}$. The oxygen substoichiometry x was not measured by this study. However, the onset of the critical transition temperature T_c onset was measured (discussed later) and it was found that T_c onset > 90 K. Cava *et al.*¹⁰ measured T_c versus x for pure $\text{YBa}_2\text{Cu}_3\text{O}_{7-x}$, and their results imply that the bulk average value of the oxygen content is probably $x < 0.1$ in this experiment. Small amounts of second phase material were evident using x-ray powder diffraction and a second discontinuous phase was observed between HTSC grains in partially polarized optical micrographs. This second phase amounts to less than 5% by volume. Hereafter, $\text{Y}_{0.9}\text{Gd}_{0.1}\text{Ba}_2\text{Cu}_3\text{O}_{7-x}$ will be abbreviated YGdBCO.

The sintered YGdBCO pellets were repulverized for neutron irradiation using a mortar and pestle. The HTSC powder was dispersed onto an aluminum plate with a 125- μm depression machined in it. This shallow depression insured that the neutron flux at the sample center was not greatly diminished by the strong absorption effects in the Gd-containing HTSC material. Another aluminum plate was clamped on top and this entire sandwich placed in a cylindrical aluminum canister. The canister was then cold welded in preparation for irradiation.

Pure $\text{GdBa}_2\text{Cu}_3\text{O}_{7-x}$ sintered pellets were also prepared for this study. $\text{GdBa}_2\text{Cu}_3\text{O}_{7-x}$ will be abbreviated GdBCO from now on. The bulk GdBCO samples were thinned on diamond impregnated papers to produce slabs with thicknesses of either ~ 100 or ~ 300 μm (the former for thermal-neutron irradiations, the latter for fast-neutron irradiations). These slabs were then wrapped in aluminum foil and placed in aluminum canis-

ters. A separate sample was prepared for each irradiation, with HTSC masses ranging from 10–200 mg.

Neutron irradiations were carried out in three different irradiation positions at the Omega West reactor at Los Alamos National Laboratory: (i) a *thermal* spectrum port, consisting of a thermal (< 10 eV) flux of 3.4×10^{12} $n_{\text{th}}/\text{cm}^2\text{s}$ and a fast (> 0.1 MeV) flux of 2.7×10^{10} $n_f/\text{cm}^2\text{s}$; (ii) a *fast* spectrum port consisting of a thermal flux of $\leq 10^8$ $n_{\text{th}}/\text{cm}^2\text{s}$ and a fast flux of 4×10^{12} $n_f/\text{cm}^2\text{s}$; and (iii) a *mixed* spectrum port, consisting of a thermal flux of 4×10^{13} $n_{\text{th}}/\text{cm}^2\text{s}$ and a fast flux of 4×10^{13} $n_f/\text{cm}^2\text{s}$. The fast-neutron flux [i.e., the integrated neutron flux above the Cd cutoff at 0.5 eV (Ref. 11)] in the thermal port was estimated based on a value for the Cd_{Au} ratio of 9.0.¹² The temperatures during irradiations were $\sim 50^\circ\text{C}$, $\sim 75^\circ\text{C}$, and $\sim 60^\circ\text{C}$ for the thermal-, fast-, and mixed-neutron irradiations, respectively. All neutron flux values reported here refer to the neutron flux at full reactor power, which is 8 MW at Omega West.

Superconducting properties of the unirradiated and irradiated samples were determined with a Quantum Design Model MPMS SQUID Magnetometer, which has range capabilities of 1.8 to 380 K and 0 to ± 55 kOe. The powder samples were packed into plastic drinking straws and confined between small pieces of quartz wool. Zero-field-cooled and field-cooled susceptibilities were measured at 10 Oe as a function of temperature. The superconducting transition onset (the first diamagnetic deviation from the normal-state susceptibility) and midpoint (the temperature at which the susceptibility is $\frac{1}{2}$ of the 7 K value) were determined from the zero-field-cooled data. Magnetization curves were obtained at 7, 25, 45, and 75 K after cooling first in zero-field to the measuring temperature and then ramping the field to maximum values of ± 50 kOe, so as to trace out a complete hysteresis loop.

EXPECTED THERMAL-NEUTRON EFFECTS

The kinetic energy of a recoiling Gd nucleus in a radiative (n, γ) capture event may be estimated using conservation of momentum. The recoil is the sum of the “kick” caused by the incident neutron and the kicks due to the emission of all subsequent photons (typically several γ photons are emitted per capture). To calculate the mean recoil energy $\langle T \rangle$ it is assumed that the emission of γ rays is isotropic and uncorrelated.¹³ Then the photon component of recoil depends on the average of the square of the gamma-ray energy E_γ^2 over the entire photon emission spectrum

$$\langle T \rangle \approx \frac{1}{1+A} E_n + \frac{\langle E_\gamma^2 \rangle}{2(1+A)m_u}, \quad (1)$$

where $\langle T \rangle$ is the average recoil energy of the nucleus after (n, γ) decay, A is the atomic weight of the target nucleus in atomic mass units (amu), E_n is the energy of the incoming neutron, and $m_u = 931.494$ MeV/amu is the energy equivalence constant for one atomic mass unit. The leading term, which represents kinetic-energy transfer to the target nucleus by the incident neutron, is

negligible for thermal neutrons. For the ^{157}Gd nucleon, which possesses the highest thermal-neutron capture cross section of all isotopes [$\sigma_\gamma = 2.55 \times 10^5$ b (Ref. 14)], the mean recoil energy of the transmuted ^{158}Gd daughter is 34 eV [determined using Eq. (1) and the γ -ray emission spectrum for ^{158}Gd (Ref. 15)]. Likewise, the same analysis reveals that the mean recoil energy of the transmuted ^{156}Gd daughter of the ^{155}Gd nucleon [$\sigma_\gamma = 6.1 \times 10^4$ b (Ref. 14)] is 29 eV. These two reactions are singled out because ^{155}Gd and ^{157}Gd account for 99.99% of all neutron capture reactions in this material.

These calculated recoil energies are close to typical displacement threshold energies in many engineering materials, i.e., $E_d \sim 25$ eV.¹⁶ If one accepts a displacement threshold energy of $E_d = 25$ eV for Gd, and employs a Kinchin-Pease model¹⁷ to determine the number of secondary displaced ions $\nu(T)$ per primary (n, γ) reaction, one concludes that on average only *one* ion is displaced per reaction, that being the primary knock-on Gd ion. Thus a Frenkel pair defect on the Gd sublattice is produced with each (n, γ) reaction. The consequence of neutron capture reactions is a largely undisturbed crystalline lattice with randomly distributed Frenkel pair defects on the Gd sublattice.

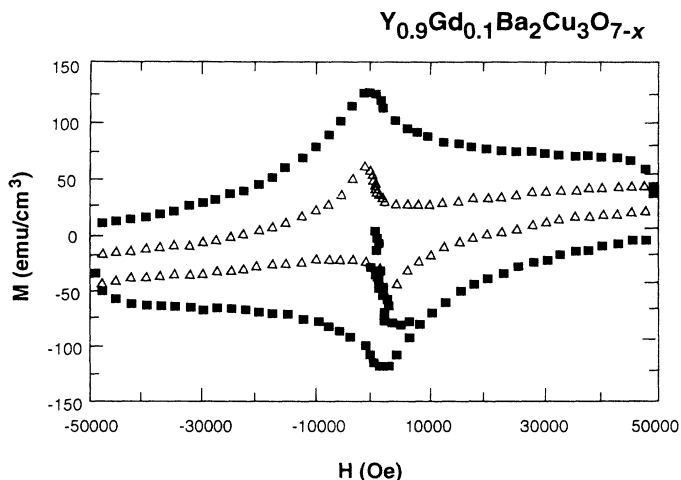
RESULTS

YGdBCO: Mixed-neutron spectrum irradiations

Figure 1 shows the sample volume magnetization M measured at $T = 7$ K plotted versus applied magnetic field H_a for unirradiated YGdBCO and the same material irradiated to a total neutron fluence of 2×10^{18} n/cm^2 . Sample magnetization measurements were also carried out at three higher temperatures (25, 45, and 75 K) and on samples irradiated to seven different fluences.

The irreversibility or hysteresis, the difference in M between increasing and decreasing branches of the magnetization curve, is attributed to the presence of flux-pinning sites in the material.¹⁸ Flux pinning allows the establishment of magnetic-flux gradients as H_a is varied. By Ampere’s law, these flux gradients are accompanied by a current density J . Within the critical-state model of Bean,¹⁹ each volume of material that has developed a flux gradient is assumed to carry the maximum possible (critical) current density J_c , consistent with the strength of the pinning present. With the further assumption that J_c is independent of H_a , the magnetization data here may be easily analyzed to obtain values of J_c . For the simplest case of a long thin cylinder oriented parallel to the applied field, the critical-current density is expressed as $J_c = 15 \Delta M/d$, where J_c is in A/cm², ΔM is the total hysteresis in emu/cm³, and d is the sample diameter in cm.²⁰ Other sample geometries involve more complex proportionality constants.²¹ The increase in the area of the hysteresis loop for the irradiated sample is attributed to an increase in J_c caused by radiation-induced defects in the lattice.^{7, 18, 21}

Figure 2 shows values of J_c at a field of $H_a = 10$ kOe for YGdBCO as a function of neutron fluence as determined from the above analysis. The value of $1.46 \mu\text{m}$



△ Unirradiated
■ Neutron irradiated

Total neutron fluence
Thermal-neutron fluence
Fast-neutron fluence

$\Phi t = 2 \times 10^{18} \text{ n/cm}^2$
 $\Phi_{th} t = 1 \times 10^{18} \text{ n}_{th}/\text{cm}^2$
 $\Phi_f t = 1 \times 10^{18} \text{ n}_f/\text{cm}^2$

FIG. 1. Magnetization M as a function of applied magnetic field H_a as measured at $T=7$ K for unirradiated $\text{Y}_{0.9}\text{Gd}_{0.1}\text{Ba}_2\text{Cu}_3\text{O}_{7-x}$ and for the same material irradiated to a total neutron fluence of $2 \times 10^{18} \text{ n/cm}^2$. This irradiation took place in the South Beam Port of the Omega West Reactor, a mixed-neutron spectrum facility. The port for this irradiation is characterized by a thermal-neutron flux of $\sim 4 \times 10^{13} \text{ n}_{th}/\text{cm}^2\text{s}$ and a fast flux of $\sim 4 \times 10^{13} \text{ n}_f/\text{cm}^2\text{s}$.

used for d is the average value of the grain diameter as determined from scanning electron microscopy observations of approximately 100 grains. It is assumed here that the dominant contribution to ΔM is due to intragranular circulation currents and that any contributions from intergranular currents in multigrain particles are negligible.²¹ Due to this and other assumptions in this analysis ($J_c = \text{const}$ and the cylindrical approximation to the sample shape), the absolute magnitudes of J_c have some uncertainty, whereas the relative values are expected to be much more accurate.

These results indicate significant enhancements in the

intragranular J_c following low-dose exposure to a mixed spectrum of neutrons. The additional flux pinning from neutron irradiation increased J_c by a maximum factor of 7.5 at 10 kOe. This was observed at a total neutron fluence of $5 \times 10^{17} \text{ n/cm}^2$ at 75 K and also at a total fluence of $2 \times 10^{18} \text{ n/cm}^2$ at 45 K.

Figure 3 shows the effect of the neutron irradiations on the critical temperature T_c . Both the T_c onset and the T_c midpoint are plotted as a function of the total neutron fluence. These are with the samples zero field cooled and measured in a field of 10 Oe. The T_c onset remains virtually constant at about 92 K out to a fluence of $\sim 2 \times 10^{18} \text{ n/cm}^2$, while the T_c midpoint drops from about 85 to 83 K. Beyond $2 \times 10^{18} \text{ n/cm}^2$ fluence, both values decrease

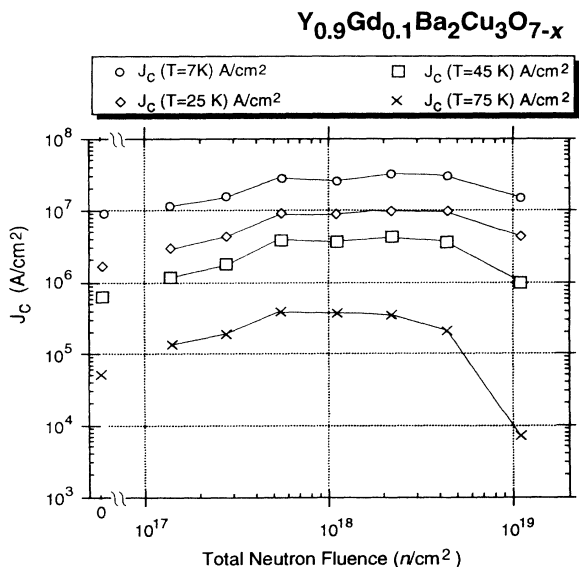


FIG. 2. Critical-current density J_c at an applied field of 10 kOe for $\text{Y}_{0.9}\text{Gd}_{0.1}\text{Ba}_2\text{Cu}_3\text{O}_{7-x}$ as a function of total neutron fluence (South Beam Port, Omega West Reactor; mixed-neutron spectrum; irradiation conditions are characterized by the same thermal and fast components as described in Fig. 1).

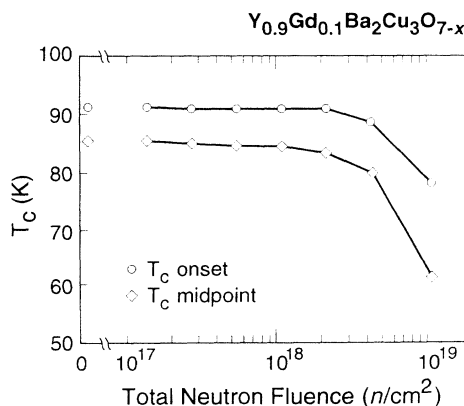


FIG. 3. Critical temperatures T_c onset and T_c midpoint (see text for description) plotted as a function of total neutron fluence (South Beam Port, Omega West Reactor; mixed-neutron spectrum; irradiation conditions are characterized by the same thermal and fast components as described in Fig. 1). Measurements were made after cooling the sample to 7 K, applying a field of 10 Oe, and measuring while warming the sample.

sharply so that T_c midpoint is only ~ 63 K at a fluence of 1×10^{19} n/cm^2 . The zero-field-cooled superconducting volume fraction varies from about 0.8 for low fluence irradiations, dropping off only for the two highest fluences to 0.6. The field-cooled volume fraction showed a similar dependence on fluence, dropping from 0.3 to 0.15. (The superconducting volume is calculated from the measured mass and the x-ray density and assuming a demagnetizing factor of $\frac{1}{3}$ for a sphere.)

Figure 4 shows the number density β_j of neutron capture reactions for ^{155}Gd , ^{157}Gd , and "all-Gd" (the latter refers to the sum of interactions with all Gd isotopes) as a function of total neutron fluence for this mixed spectrum irradiation. The number of "burn-up" reactions per cm^3 , β_j , for the j th isotope is given by $\beta_j = N_j \sigma_j \Phi t$, where N_j is the concentration of the j th isotopic reactant in cm^{-3} , σ_j is the cross section for (n, γ) neutron capture in cm^2 by that isotope, Φ is the neutron flux in n/cm^2 s, and t is the elapsed time in seconds.

Figure 5 shows the number of displacements per atom (DPA) due to neutron capture, normalized either to the total number of $^{155}\text{Gd} + ^{157}\text{Gd}$ reactants or to the total number of atoms in the YGdBCO structure, as a function of total neutron fluence. Total DPA is defined as $\beta v / N_0$,

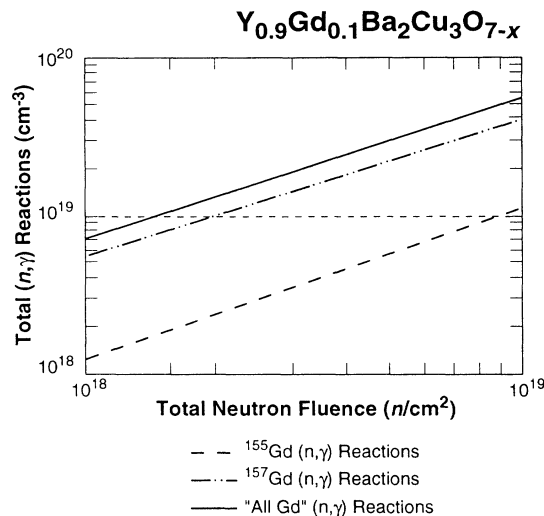


FIG. 4. Calculated number density of neutron (n, γ) capture reactions for ^{155}Gd , ^{157}Gd , and the sum of all Gd interactions, for $\text{Y}_{0.9}\text{Gd}_{0.1}\text{Ba}_2\text{Cu}_3\text{O}_{7-x}$ as a function of total neutron fluence (South Beam Port, Omega West Reactor; *mixed*-neutron spectrum; irradiation conditions are characterized by the same thermal and fast components as described in Fig. 1). The neutron spectrum for this calculation was obtained from earlier calculations (Ref. 22) using the DANDE code system (Ref. 23), which describes the fuel within a plate of an Omega West Reactor fuel assembly. The code TOAFEW-5 (Ref. 24) was then used to produce four-group integral flux values covering the neutron energy range from 10^{-5} to 10^7 eV. The code TOAFEW-5 also generates the associated four-group flux-weighted average cross sections needed for the burn-up calculation. Finally, the number of reactions per cm^3 as a function of irradiation time was calculated using the CINDER-2 code (Ref. 25).

where β is the (n, γ) reaction density summed over all Gd isotopes, v is the average number of secondary displacements per primary displacement [which here is taken to be *one* per (n, γ) reaction], and N_0 is the atomic density of the material. Also shown in Fig. 5 is the average spacing of defects in the crystal structure resulting from thermal neutron capture.

Using simple approximations, one can estimate fast-neutron damage and make a useful comparison with calculated neutron capture effects. Assume that $\sigma_f = 2$ b is a representative fast-neutron elastic scattering cross section¹ and assume a fast-neutron fluence $\Phi_f t = 1 \times 10^{18}$ n_f/cm^2 (the case for maximum flux-pinning enhancements at $T = 45$ K). Then one finds the fast-neutron-induced primary knock-on (PKA) density is given by $\beta_f = N_0 \sigma_f \Phi_f t = 1.5 \times 10^{17}$ cm^{-3} . From Fig. 4, the (n, γ) reaction density at this fluence is about 1.5×10^{19} cm^{-3} , suggesting that the PKA/ (n, γ) reaction density ratio is $\sim 1/100$. (The fast-neutron fluence of interest here is 1×10^{18} n_f/cm^2 ; the total neutron fluence is twice this value, i.e., 2×10^{18} n/cm^2 , since the fast-neutron flux represents about half the total flux in the *mixed*-spectrum irradiation position.)

Each PKA ion produces a cascade or displacement spike that consists of numerous secondary displaced ions. The details of such cascades were examined by computer simulation using the Monte Carlo code TRIM.²⁶ PKA

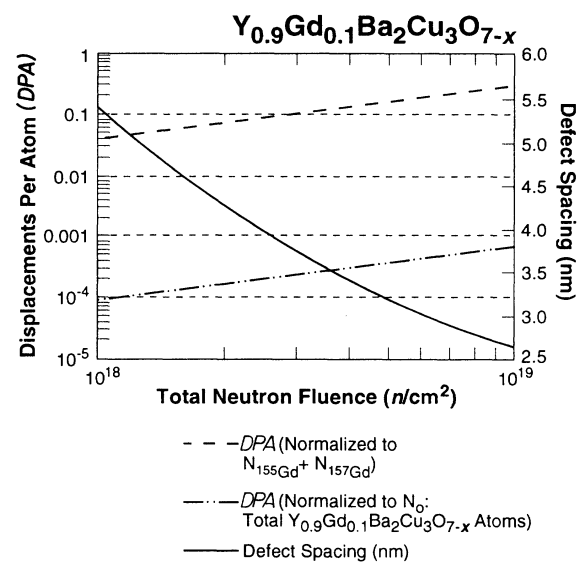


FIG. 5. Calculated number of displacements per atom (DPA) due to neutron (n, γ) capture events, normalized to either the total number of $^{155}\text{Gd} + ^{157}\text{Gd}$ reactants or the total number of atoms in $\text{Y}_{0.9}\text{Gd}_{0.1}\text{Ba}_2\text{Cu}_3\text{O}_{7-x}$, as a function of total neutron fluence (South Beam Port, Omega West Reactor; *mixed* spectrum; irradiation conditions are characterized by the same thermal and fast components as described in Fig. 1). Also shown is the average spacing of defects in the crystal structure resulting from neutron capture, assuming the Frenkel pair defect mechanism discussed in the text (a Frenkel pair is counted as one defect). Furthermore, it is assumed that all thermal-neutron capture events on the Gd sublattice lead to the production of Frenkel pairs and that all of these point defects survive.

cascade simulations reveal that a large distribution is to be expected for $\nu(T)$, the average number of secondary displacements per PKA displacement. If ν is taken to be 5×10^2 (based on TRIM results), then the total DPA due to fast neutrons for the fluence considered here is 10^{-3} . Though fast-neutron-induced defects are significantly less abundant in the lattice than thermal-neutron-induced defects, this result suggests that the total lattice damage attributable to fast neutrons in this experiment is greater than that due to thermals by about a factor of 10.

It is more difficult to estimate the size and spacing of fast-neutron-induced defects that may actually be responsible for flux pinning. In the simple terms of displaced atom counts, fast-neutron-induced cascade defects are larger than (n, γ) reaction defects. But cascades are made up of subcascades, i.e., point defect clusters linked by damaged matrix material (e.g., see Thompson²⁷). In a simulation such as TRIM, these appear as "lobes" adjacent to the path denoting the PKA trajectory. They can range in size from just a few displaced atoms to hundreds of vacancies and interstitials. For low-energy PKA's with short range, subcascades are spatially close and the PKA cascade can be treated as a single entity. TRIM results indicate, for example, that within the longitudinal range of a 3-keV Gd PKA (~ 3 nm), only one or two subcascades consisting of more than 10 point defects are produced per PKA (these subcascades are initiated by secondary knock-on ions). But in the case of high-energy PKA's, spatially distinct subcascades are more apparent

in TRIM simulations. For instance, the longitudinal range of a 61-keV Cu PKA is about 30 nm. TRIM results indicate that along this extended range, at least 10 subcascades are typically present, consisting of more than 10 point defects, and 2–3 of these subcascades contain more than 100 vacancies and interstitials.

In summary, fast-neutron-induced PKA defects are extended and widely spaced compared to the closely spaced thermal-neutron-induced Frenkel pair defects. But PKA cascades are complicated by a wide distribution of sizes and substructure. It is not possible to estimate the size and spacing of fast-neutron-induced defects that may play a role as flux-pinning centers. Also, at this stage, whether or not thermal-neutron-induced defects, fast-neutron-induced defects, or both, play a role as flux-pinning defects, is not clear. The next section describes an experiment that addresses this issue.

GdBCO: Thermal- and fast-neutron spectra irradiations

To determine the defects responsible for flux-pinning enhancements in the YGdBCO material, an experiment was designed to separate thermal- and fast-neutron effects. GdBCO was selected for this study to ease somewhat the chemical complications associated with multicomponent materials. As described in the experimental procedure, bulk slabs of GdBCO were exposed either to primarily thermal-neutron, or alternatively, primarily fast-neutron environments. Exposures were designed to

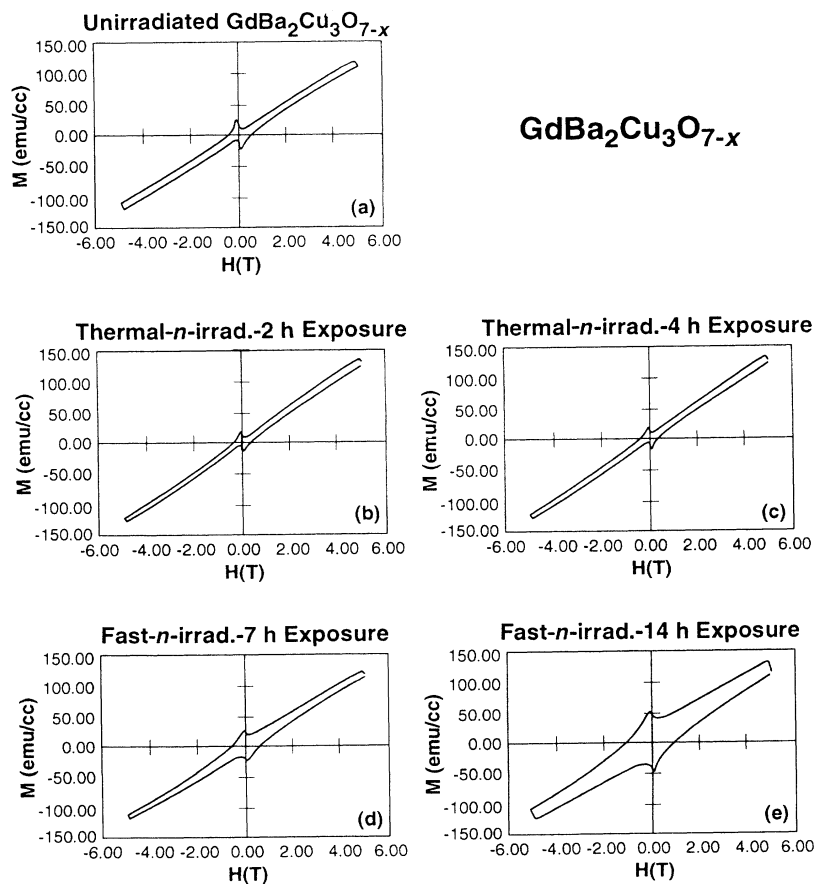


FIG. 6. Magnetization M as a function of applied magnetic field H_a (measured at $T = 20$ K) for (a) unirradiated $\text{GdBa}_2\text{Cu}_3\text{O}_{7-x}$ (GdBCO); (b) GdBCO irradiated in a *thermal*-neutron spectrum (TCR-1, Omega West Reactor) to an exposure of 2 h (thermal-neutron fluence = $2.5 \times 10^{16} n_{th}/\text{cm}^2$); (c) same as (b) except exposure = 4 h (thermal-neutron fluence = $5 \times 10^{16} n_{th}/\text{cm}^2$); (d) GdBCO irradiated in a *fast*-neutron spectrum (North Vertical Port, Omega West Reactor) to an exposure of 7 h (fast-neutron fluence = $1 \times 10^{17} n_f/\text{cm}^2$); (e) same as (d) except exposure = 14 h (fast-neutron fluence = $2 \times 10^{17} n_f/\text{cm}^2$).

achieve similar levels of damage in the material with either irradiation source, based on qualitative estimates for the number of displacements per atom.

The fluences for the thermal-neutron irradiations were designed to yield approximately the same thermal-neutron DPA as was estimated for the case of maximum flux-pinning enhancements in YGdBCO (at 45 K), i.e., DPA $\sim 10^{-4}$. To achieve 10^{-4} DPA in a thermal-neutron experiment using GdBCO requires less fluence than for YGdBCO, since the Gd isotope concentrations are all higher by a factor of 10. From the flux component values of the thermalized irradiation port (see Experimental Procedure section), and the corresponding neutron capture cross sections, one finds an (n, γ) reaction rate of $1 \times 10^{15} \text{ cm}^{-3} \text{ s}^{-1}$. Taking $\nu=1$, the damage accumulation rate in this experiment is $\sim 10^{-8}$ DPA/s. So an exposure of 10^4 s (2.8 h) satisfies the damage level requirement of 10^{-4} DPA.

A fast-neutron fluence yielding an equivalent damage level was estimated as follows. It is often found for ceramics that damage accumulation rates for fast neutrons ($E_n > 0.1 \text{ MeV}$) are of the order of 1 DPA per $10^{21} n_f/\text{cm}^2$ (see, e.g., Refs. 2, 28, and 29). Using this assumption and the flux component values for the fast-neutron-predominating port, the damage accumulation rate was estimated to be $\sim 4 \times 10^{-9}$ DPA/s. So, an exposure of $2.5 \times 10^4 \text{ s}$ (7 h) should produce a damage level of $\sim 10^{-4}$ DPA.

Based on these estimates, GdBCO slabs were exposed for 2 h and 4 h, respectively, in the thermal-neutron irradiation facility (2.5×10^{16} and $5 \times 10^{16} n_{\text{th}}/\text{cm}^2$), and for 7 h and 14 h, respectively, in the fast-neutron irradiation facility (1×10^{17} and $2 \times 10^{17} n_f/\text{cm}^2$). These irradiations were intended to examine the range 1×10^{-4} – 2×10^{-4} DPA for both thermal- and fast-neutron experiments.

Figure 6 shows the results of sample magnetization measurements on each of the irradiated bulk GdBCO samples described here, as well as on an unirradiated sample. These measurements were made at 20 K, though similar results were obtained at 50 K. An expansion in the hysteresis loop is observed for both the fast-neutron-irradiated samples compared to the unirradiated sample. On the other hand, no measured expansion occurs in either of the thermal-neutron-irradiated samples. The hysteresis ΔM as measured at $H_a = 20 \text{ kOe}$, is increased by a factor of 3 for the long-exposure fast-neutron-irradiated sample, while ΔM in the case of the long-exposure thermal-neutron sample, if anything, is decreased slightly.

These results indicate that flux pinning and therefore critical-current (J_c) enhancements in GdBCO are attributable to fast-neutron and not to thermal-neutron-induced defects. It seems reasonable to conclude that the implications of these results extend to flux-pinning effects in YGdBCO as well.

DISCUSSION

Fast-neutron-induced cascade-type defects have been shown here clearly to be responsible for flux pinning and

intrinsic critical-current enhancements in Gd-containing HTSC barium cuprates. Previous work has already demonstrated that fast neutrons are effective at inducing flux-pinning defects in yttrium barium cuprate. For example, Cost *et al.*¹ found J_c enhancements following fast-neutron irradiation of polycrystalline $\text{YBa}_2\text{Cu}_3\text{O}_{7-x}$ (YBCO). At their highest fluence of $1 \times 10^{18} n_f/\text{cm}^2$ ($E_n > 0.1 \text{ MeV}$), they found a 9.5 times enhancement in J_c at $T = 7 \text{ K}$, as measured at $H_a = 10 \text{ kOe}$. Again, assuming a 2 b cross section for elastic scattering, the spacing of primary collision events at this fluence is about 19 nm, the same as the fast-neutron-induced PKA defect spacing in this experiment (at the fluence corresponding to the maximum observed flux-pinning enhancements).

Thermal neutrons have also been shown previously to produce effective flux-pinning lattice defects. An experiment by Fleisher *et al.*²¹ used thermal neutrons to produce defects in polycrystalline ^{235}U -doped YBCO. In this case, defects are initiated by neutron capture and subsequent fission of ^{235}U nuclei. The maximum internal concentration of fission events in this experiment was $5 \times 10^{14} \text{ cm}^{-3}$, which corresponds to an average fission-track spacing of 130 nm. Though much larger than the calculated PKA cascade or Frenkel pair spacings in this experiment, Fleisher *et al.* observed a 12 times enhancement in J_c at $T = 63 \text{ K}$ as measured at $H_a = 10 \text{ kOe}$. Fission-induced defects are somewhat akin to fast-neutron-induced defects in that both mechanisms produce damage (with substructure) over an extended volume. These published results as well as those presented here indicate that spatially extended neutron-induced defects in YBCO or Gd-substituted YBCO, can act as effective flux-pinning sites.

The question that remains unanswered is do Frenkel pair point defects exist following thermal-neutron irradiations of Gd-doped HTSC materials? Or is their formation suppressed due to the fact that the threshold energy for formation E_d is significantly greater than $\sim 30 \text{ eV}$ [based on the average impulse to a recoiling Gd ion in an (n, γ) reaction]? Or are they annihilated by recombination processes at irradiation temperatures that under the experimental conditions employed here are noncryogenic?

The proposed existence of point defects or Frenkel pairs in the thermal-neutron-irradiated materials has not been proven. Some evidence for the existence of defects is available, however. Brezgunov *et al.*³⁰ and Makletsov³¹ have demonstrated that the thermal component of a reactor neutron spectrum is highly effective in altering superconducting properties in GdBCO. They examined the influence of thermal neutrons on the damage response of polycrystalline GdBCO by comparing the decrease in T_c due to fast-neutron exposure to T_c degradation following exposure to a mixed-neutron spectrum (containing a substantial thermal component $\Phi_{\text{th}}/\Phi_f \sim 4$). These researchers found that the mixed-spectrum fluence necessary to decrease T_c to one-half its unirradiated value ($5.2 \times 10^{18} n/\text{cm}^2$) was only 40% of the fast-neutron fluence needed to reduce T_c by one half ($1.3 \times 10^{19} n_f/\text{cm}^2$).

Table I shows results of T_c -onset and T_c -midpoint

TABLE I. Effects of thermal-neutron and fast-neutron irradiations on the critical transition temperature in bulk $\text{GdBa}_2\text{Cu}_3\text{O}_{7-x}$.

| Sample | n fluence | T_c onset | T_c midpoint | ΔT_c midpoint $10^{17} n/\text{cm}^2$ ^a |
|--|--|-------------|----------------|---|
| Unirradiated | | 91 K | 74 K | |
| Thermal-neutron-irradiated 2-h exposure | $2.5 \times 10^{16} n_{\text{th}}/\text{cm}^2$ | 90 K | 58 K | 64 K |
| Thermal-neutron-irradiated 4-h exposure | $5 \times 10^{16} n_{\text{th}}/\text{cm}^2$ | 90 K | 59 K | 30 K |
| Fast-neutron-irradiated 7-h exposure | $1 \times 10^{17} n_f/\text{cm}^2$ | 91 K | 72 K | 2 K |
| Fast-neutron-irradiated 14-h exposure | $2 \times 10^{17} n_f/\text{cm}^2$ | 90 K | 61 K | 13 K |

^aThe numbers in this column are based on linear extrapolation, taking individually each measured T_c -midpoint value. Each value is normalized to 10^{17} total neutrons (thermal + fast) per cm^2 .

measurements on GdBCO samples exposed either to thermal or fast neutrons in our experiment. These measurements were made by precisely the same procedures used for the YGdBCO samples (Fig. 3). The T_c midpoint diminishes at a rate of 64 K per $10^{17} n_{\text{th}}/\text{cm}^2$ (linear approximation) for a 2 h exposure in the thermal-neutron facility, while only falling 2 K per $10^{17} n_f/\text{cm}^2$ for a 7 h fast-neutron exposure (linear approximation). (Results indicate that the linear extrapolation used here is valid neither for thermal or fast neutrons. The degradation in T_c midpoint seems to have saturated by $2.5 \times 10^{16} n_{\text{th}}/\text{cm}^2$ thermal-neutron exposure, while the T_c degradation rate is still increasing for fast-neutron exposures beyond $10^{17} n_f/\text{cm}^2$.) These results verify that thermal neutrons exhibit a stronger influence on T_c degradation than fast neutrons.

The observation of T_c degradation in the thermal-neutron-irradiated GdBCO samples may be indirect evidence for the presence of defects such as the proposed Frenkel pairs on the rare-earth sublattice. At the very least, these results imply that lattice distortions are induced by thermal neutrons that do not anneal out (or that are maintained) at temperatures at or below the irradiation temperature.

In summary, thermal-neutron-induced defects are not effective flux-pinning centers in GdBCO. The existence of Frenkel-pair-type point defects on the rare-earth sublattice is proposed here, but evidence for such defects is not conclusive. If these point defects do exist, then results presented here indicate that they are not effective pinning centers for magnetic flux in HTSC barium cuprate materials.

This is intriguing because other work by Seuntjens, Daeumling, and Larbalestier,³² particularly related to non-stoichiometric oxides, has indicated that point defects on the oxygen sublattice are effective pinning sites for magnetic flux. Seuntjens, Daeumling, and Larbales-

tier propose that point defects due to oxygen substoichiometry disrupt the ordered oxygen structure in the orthorhombic superconducting material, and in so doing serve as strong magnetic-flux-pinning defects. This proposition seems to be theoretically justified. It is presumed³³ that to optimally pin magnetic flux, defect size should be comparable to the radius of a fluxon's normal core, i.e., the coherence length. In YBCO, the coherence lengths ξ_{ab} and ξ_c in the a - b plane and along the c direction, respectively, have been estimated to range from $0.5 \text{ nm} < \xi_{ab} < 1.5 \text{ nm}$ and $0.1 \text{ nm} < \xi_c < 0.5 \text{ nm}$.³⁴ The displacement field of a vacancy on the oxygen sublattice, or for that matter of an (n, γ) -reaction-induced Frenkel pair on the rare-earth sublattice, probably lies within this range. (Many subcascades within fast-neutron-induced PKA damage volumes are also likely to satisfy this criterion.) But the results presented here may indicate that this size criterion is not a sufficient condition for effective magnetic-flux pinning.

The damage to the superconductor, that is, the modification of the superconducting order parameter, is expected to be much stronger if the defect or Frenkel pair involves the Cu-O plane. This is because the Cu-O plane is the part of the structure that is considered to be most critical for the presence of superconductivity. Thus it may not only be the size of the defect, but also its location that affects flux pinning.

The existence of isolated point defects or Frenkel pairs following (n, γ) reactions in YGdBCO or GdBCO remains an open question. Work is in progress to verify the absence or presence of point defects in thermal-neutron-irradiated, Gd-doped, and other rare-earth-doped HTSC's.

CONCLUSIONS

Neutron irradiations of $\text{Y}_{0.9}\text{Gd}_{0.1}\text{Ba}_2\text{Cu}_3\text{O}_{7-x}$ were carried out to fluences ranging from 1×10^{17} to 1×10^{19}

n/cm^2 in a mixed-spectrum reactor. The neutron spectrum in this experiment was divided approximately equally between thermal ($\Phi[E_n < 0.5 \text{ eV}]$) and epithermal and fast ($\Phi[E_n > 0.5 \text{ eV}]$) components. Neutron (n, γ) capture reactions on the Gd sublattice accounted for a substantial fraction of damage events during irradiation. Critical-current density J_c was found to increase for total neutron fluences ranging between $1 \times 10^{17} - 2 \times 10^{18} n/\text{cm}^2$, relative to the unirradiated value. The maximum observed enhancement in J_c was about a factor of 7.5. This occurred at a total neutron fluence of $5 \times 10^{17} n/\text{cm}^2$ ($T = 75 \text{ K}$; $H_a = 10 \text{ kOe}$) and at a neutron fluence of $2 \times 10^{18} n/\text{cm}^2$ ($T = 45 \text{ K}$; $H_a = 10 \text{ kOe}$).

Neutron irradiations of bulk $\text{GdBa}_2\text{Cu}_3\text{O}_{7-x}$ were carried out in highly thermalized or pure fast irradiation positions (in the same reactor) to determine if enhancements in J_c are to be attributed to defects arising from interactions with thermal neutrons ($E_n \sim 0.025 \text{ eV}$) or with fast neutrons ($E_n > 0.1 \text{ MeV}$). Thermal neutrons interact strongly with the Gd nuclei in the structure, resulting in the probable displacement of Gd ions from their lattice sites. On average, no secondary displacements are incurred in this process, leaving simply an accumulation of Frenkel pair defects on the Gd sublattice. Fast neutrons, on the other hand, produce cascade and subcascade structures, consisting of a broad size distribution of point defect clusters. Fluences selected for both the thermal and fast neutron irradiations were designed to examine effects at an absorbed dose of $\sim 10^{-4}$ displacements per atom DPA.

Magnetization measurements (M versus H_a) on these samples indicated that flux pinning (and thereby J_c) was enhanced by fast-neutron irradiation, but not by thermal-neutron irradiation. These results suggest that if point defects on the rare-earth sublattice exist following exposure to thermal neutrons, these point defects do not serve as effective flux-pinning centers.

Measurements of T_c on the bulk $\text{GdBa}_2\text{Cu}_3\text{O}_{7-x}$ samples showed that T_c is degraded by both thermal and fast neutrons and a higher rate of T_c degradation was observed for thermal-neutron exposures compared to fast-neutron exposures. The T_c midpoint diminishes at a rate of $64 \text{ K per } 10^{17} n_{\text{th}}/\text{cm}^2$ (linear approximation) for a thermal-neutron-exposed sample, compared to $2 \text{ K per } 10^{17} n_f/\text{cm}^2$ for a fast-neutron-exposed sample (linear approximation). Thermal-neutron-irradiation effects on T_c seem to verify that lattice disorder is induced by the (n, γ) capture process.

ACKNOWLEDGMENTS

This work was supported by the Department of Energy, Office of Basic Energy Sciences, and through the Exploratory Research and Development Center (J.O.W., P.J.K., and M.P.M.). Special thanks are due to D. E. Peterson and Z. Fisk for producing the materials for this study, to C. D. Kise and G. F. Ramsey for technical assistance at the Omega West facility, and to S. G. Boeke, W. A. Coghlan, and M. M. Chadwick for additional laboratory and computational assistance.

*Also at Superconductivity Research Laboratory, 10-13 Shinonome 1-chome, Koto-ku, Tokyo 135, Japan.

- ¹J. R. Cost, J. O. Willis, J. D. Thompson, and D. E. Peterson, *Phys. Rev. B* **37**, 1563 (1988); J. O. Willis, J. R. Cost, R. D. Brown, J. D. Thompson, and D. E. Peterson, in *High Temperature Superconductors*, edited by M. B. Brodsky, R. C. Dynes, K. Kitazawa, and H. L. Tuller, MRS Symposia Proceedings No. 99 (Materials Research Society, Pittsburgh, 1988), p. 391.
- ²M. A. Kirk, M. C. Frischherz, J. Z. Liu, L. R. Greenwood, and H. W. Weber, *Philos. Mag. Lett.* **62**, 41 (1990).
- ³A. Umezawa, G. W. Crabtree, J. Z. Liu, H. W. Weber, W. K. Kwok, L. H. Nunez, T. J. Moran, and C. H. Sowers, *Phys. Rev. B* **36**, 7151 (1987).
- ⁴H. W. Weber, *Physica C* **185-189**, 309 (1991).
- ⁵F. M. Sauerzopf, H. P. Weisinger, W. Kritschka, H. W. Weber, G. W. Crabtree, and J. Z. Liu, *Phys. Rev. B* **43**, 3091 (1991).
- ⁶R. B. van Dover, E. M. Gyorgy, L. F. Schneemeyer, J. W. Mitchell, K. V. Rao, R. Puzniak, and J. V. Waszczak, *Nature* **342**, 55 (1989).
- ⁷A. R. Sweedler, D. E. Cox, and S. Moehlecke, *J. Nucl. Mater.* **72**, 50 (1978).
- ⁸P. Muller, W. Schindler, G. Saemann-Ischenko, H. Burzclaff, H. Gerstenberg, and M. Fisher, *Physica C* **153-155**, 343 (1988).
- ⁹*Neutron Cross Sections*, Vol. 1, edited by S. F. Mughabghab, R. R. Kinsey, and C. L. Dunford (Academic, New York, 1981).
- ¹⁰R. J. Cava, A. W. Hewat, E. A. Hewat, B. Batlogg, M. Marezio, K. M. Rabe, J. J. Krajewski, W. F. Peck, Jr., and L. W. Rupp, Jr., *Physica C* **165**, 419 (1990).
- ¹¹S. Glasstone and M. C. Edlund, *The Elements of Nuclear*

Reactor Theory (Van Nostrand, Princeton, 1952).

- ¹²M. M. Minor (unpublished).
- ¹³R. E. MacFarlane, D. W. Muir, and R. M. Boicourt (unpublished).
- ¹⁴*Nuclides and Isotopes*, 14th ed., revised by F. W. Walker, J. R. Parrington, and F. Feiner (General Electric Company, Nuclear Energy Operations, San Jose, CA, 1989).
- ¹⁵*Atlas of X-ray Spectra From Radiative Capture of Thermal Neutrons*, edited by L. V. Groshev, V. N. Lutsenko, A. M. Demidov, and V. I. Pelekhov, translated by J. B. Sykes (Pergamon, London, 1959).
- ¹⁶B. T. Kelly, *Irradiation Damage to Solids* (Pergamon, London, 1966), p. 2.
- ¹⁷G. H. Kinchin and R. S. Pease, *Rep. Prog. Phys.* **18**, 1 (1955).
- ¹⁸A. R. Sweedler, C. L. Snead, Jr., and D. E. Cox, *Metallurgy of Superconducting Materials*, edited by T. Luhman and D. Dew-Hughes (Academic, New York, 1979), p. 349.
- ¹⁹C. P. Bean, *Phys. Rev. Lett.* **8**, 250 (1962).
- ²⁰W. A. Fietz and W. W. Webb, *Phys. Rev.* **178**, 657 (1969).
- ²¹R. L. Fleischer, H. R. Hart, Jr., K. W. Lay, and F. E. Luborsky, *Phys. Rev. B* **40**, 2163 (1989).
- ²²W. B. Wilson, T. R. England, D. C. George, and R. J. LaBauve (unpublished).
- ²³R. J. LaBauve, T. R. England, D. C. George, R. E. MacFarlane, and W. B. Wilson, *Nucl. Sci. Eng.* **95**, 152 (1987).
- ²⁴W. B. Wilson, T. R. England, R. J. LaBauve, and R. M. Boicourt (unpublished).
- ²⁵W. B. Wilson, T. R. England, R. J. LaBauve, and J. A. Mitchell, *Nuclear Saf.* **29**, 177 (1988).

- ²⁶J. F. Ziegler, J. P. Biersack, and U. Littmark, *The Stopping and Range of Ions in Solids*, Vol. 1 of *The Stopping and Range of Ions in Matter*, edited by J. F. Ziegler (Pergamon, New York, 1985).
- ²⁷M. W. Thompson, *Defects and Radiation in Metals* (Cambridge University, Cambridge, England, 1969).
- ²⁸G. P. Pells, *J. Nucl. Mater.* **184**, 183 (1991).
- ²⁹W. A. Coghlan, F. W. Clinard, Jr., N. Itoh, and L. R. Greenwood, *J. Nucl. Mater.* **141-143**, 382 (1986).
- ³⁰M. M. Brezgunov, S. V. Belogurov, A. E. Petrov, A. N. Karpov, I. V. Kudrenitskis, V. N. Kovalev, E. N. Kurkin, A. A. Makletsov, Yu. G. Morozov, and M. D. Nersesyan, *Superconductivity* **3**, 843 (1990).
- ³¹A. A. Makletsov, *Superconductivity* **3**, 849 (1990).
- ³²J. M. Seuntjens, M. Daeumling, and D. C. Larbalestier, *Nature* **346**, 332 (1990).
- ³³A. M. Campbell and J. E. Evetts, *Critical Currents in Superconductors* (Taylor and Francis, London, 1972).
- ³⁴G. Deutscher, in *Earlier and Recent Aspects of Superconductivity*, edited by J. G. Bednorz and K. A. Müller, Springer Series in Solid State Sciences Vol. 90 (Springer-Verlag, Berlin, 1990), p. 174.